MODELLING OF IMBIBITION RELATIVE PERMEABILITY BY DIRECT QUASI-STATIC APPROACH

S. Berg[1], M. Rücker[1,2], H. Ott[1,3], A. Georgiadis[1], H. van der Linde[1], F. Enzmann[2], M. Kersten[2], R. T. Armstrong[4], S. de With[1,5], J. Becker[6], A. Wiegmann[6]

[1]Shell Global Solutions International B.V., Rijswijk, The Netherlands
[2]Geosciences Institute, Johannes Gutenberg University, Mainz, Germany
[3]Department of Petroleum Engineering, Montanuniversität Leoben, Austria
[4]School of Petroleum Engineering, University of New South Wales, Sydney, Australia
[5]Technical University of Delft, The Netherlands
[6]Math2Market GmbH, Stiftsplatz 5, 67655 Kaiserslautern, Germany

This paper was prepared for presentation at the International Symposium of the Society of Core Analysts held in Snowmass, Colorado, USA, 21-26 August 2016

ABSTRACT

Relative permeability from a quasi-static pore scale modelling approach conducted directly on the pore space of rock have been compared with relative permeability computed from 3D fluid distributions obtained from a 2-phase flow experiment under dynamic conditions imaged with synchrotron beamline-based fast X-ray computed tomography. The comparison shows good agreement between connected pathway flow simulations conducted directly on the 3D fluid distribution obtained from the synchrotron beamline experiment on Gildehauser sandstone rock with a conventional "special core analysis" steady-state relative permeability measurement on a twin-sample. A quasi-static morphological approach to model pore scale fluid distributions, however, shows large discrepancy with the experimental data. The issue with quasi-static methods is not so much the modelling of the Navier-Stokes flow, but rather the description of the pore scale fluid configurations resulting from immiscible displacement events. Cooperative, non-local displacement events are not captured by quasi-static modeling approaches, which operate entirely in the capillary regime. Respective pore scale fluid distributions are significantly different from experimental measurements. As a consequence also the respective relative permeability is significantly different than those observed in the experiment. Therefore, ultimately only dynamic approaches are really able to correctly describe the pore scale displacements and respective pore-scale fluid configurations which are imperative for the correct description of phase connectivity, fluxes of connected and disconnected phases and ultimately relative permeability.

INTRODUCTION

Pore scale modelling has given rise to industry wide activities in the domain of Digital Rock. One of the most common applications for Digital Rock is the prediction of relative permeability. Much progress has been made since in terms of the applied methodology. Currently one of questions is whether quasi-static approaches (like quasi-static pore network modelling [8]) are describing the pore scale displacement physics sufficiently well for this purpose, or whether computationally much more costly dynamic approaches are required [9-12]. All quasi-static approaches are based on similar principles, i.e. separating a capillary-dominated step to determine pore scale fluid configuration from the viscous flow during which fluid-fluid interfaces remain static. The basic question is whether this is fundamentally permissible or not. Pore network models do not really provide the answer to this question. While the missing viscous forces during "capillary" events are compensated to some extent by displacement rules, the extraction of a network is not unique and during tuning of networks the correspondence with the underlying physical pore space is likely lost [22]. Another open question is whether the rule-based displacements or the flux computation assuming static fluid-fluid interfaces represent the more questionable assumption. In the end it could be that quasi-static pore network modelling is approximately right, or that it is fundamentally wrong but sufficient parameters are available to force a match with experimental data. Dynamic approaches that explicitly model the movement of liquid-liquid interfaces cover viscous and capillary forces simultaneously and capture naturally a wide range of pore scale displacement phenomena [4,12]. Given the high computational cost, the question arises whether fully dynamic simulations are really absolutely required to model relative permeability or are rather a "nice to have" that capture effects which are in the end not that relevant.

In order to address this question, in this work the problem is approached from another angle by using only capillary-dominated displacements without any rules, and executed directly on the pore space. It is a quasi-static pore network without a network and without rules. Relative permeability from a quasi-static pore scale modelling approach conducted directly on the pore space of rock [13-16, 29] are compared with relative permeability computed from 3D fluid distributions obtained from a 2-phase flow experiment under dynamic conditions [6,7] imaged with synchrotron beamline-based fast X-ray computed tomography [1]. In order to relate differences in relative permeability to pore scale fluid distribution, the quasi-static modelling approach acts directly on the pore space and not on an abstracted network for which such a pore-level comparison is more difficult and more ambiguous [22]. As a reference for relative permeability we consider data from a steady-state experiment on a (larger size) twin sample of the same sandstone rock [2].

METHODS AND MATERIALS

For the micro-CT flow experiments, cylindrical samples of Gildehauser outcrop sandstone rock [3] (Bentheimer formation, permeability K = 1.5 D and an average porosity ϕ=20%, strongly water-wet) of 4 mm diameter and 10 mm length (which is larger than the representative elementary volume [2]) were used. They were heat-shrunk into a polycarbonate flow cell and integrated into micro-pump setup that was mounted

onto the rotation stage of the tomography setup at the synchrotron beamline. In this way continuous fluid injection was provided without external flow lines. Details of the experiments are reported elsewhere [1,2]. For the experiments we used n-decane as non-wetting phase and brine doped with 10 wt-% cesium chloride as wetting phase, with an interfacial tension of σ=35 mN/m. Saturation of the rock with brine was followed by primary drainage where n-decane was injected at a rate of 1 ml/min reaching a non-wetting phase saturation of 78% [1]. Then the actual imbibition experiment started where brine was injected at 0.1 µl/min. This corresponds by all capillary number definitions to a capillary-dominated flow regime on the basis of the injection rate. However pore scale processes can occur at orders of magnitude higher rate where locally viscous forces dominate [1,2]. Pore scale fluid distributions were monitored by synchrotron-based fast X-ray computed micro-tomography at the TOMCAT beamline at the Swiss Light Source (SLS). Tomography was performed at a beam energy of 37 keV obtained by a multilayer monochromator. For each 3D tomography image 1500 projections were collected with a PCO.edge camera at 20 ms time intervals adding up to 45 s for each 3D image. The spatial resolution was 2.2 µm/voxel. Images were first filtered (nonlocal means) and segmented (watershed segmentation) using Avizo (FEI) where the segmented pore space from a higher quality dry scan was used as a mask such that segmentation of the fluids contained only 2 phases [2]. Results of the image processing are displayed in Figure 1.

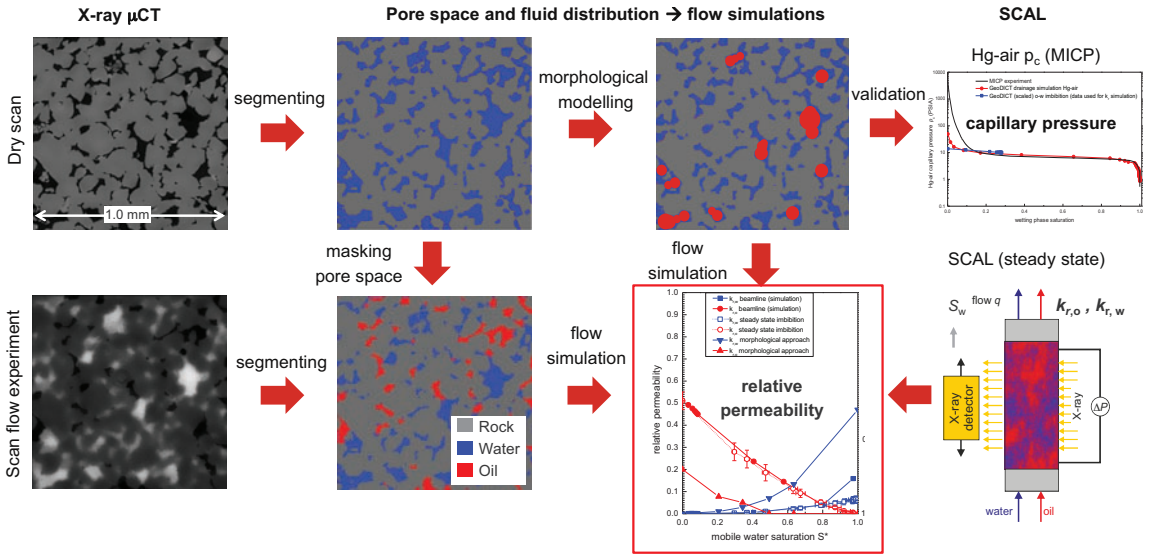

Figure 1: Workflow starting with X-ray computed tomography on the left, segmentation leading to pore space and pore scale fluid distributions, from which connected pathway relative permeability is computed. From the pore space, using a morphological approach, fluid distributions are "simulated" and after validation against capillary pressure data from MICP relative permeability is computed. For validation, steady-state SCAL experiments (right) are used.

Hydrodynamic flow simulations were conducted on the pore scale fluid distributions from µCT data at each time step and after normalization to the absolute permeability *K* (by Stokes flow simulation on the dry rock) obtaining a (connected pathway) relative

permeability. Flow simulations were conducted directly on the voxel grid of the μCT data using the SimpleFFT solver from GeoDICT (Math2Market). In addition, a morphological approach [13-16] was used to obtain pore scale fluid distributions in the capillary-dominated. The Young-Laplace equilibrium states were approximated by performing a series of erosion and dilation operations on the segmented pore space using a spherical structure element with the constraint of phase connectivity to the inlet. For drainage, the respective capillary pressure-saturation relationship was validated against mercury-air capillary pressure data obtained from mercury intrusion (MICP) showing a close match for capillary entry and plateau pressures. For imbibition the original method [13] was adapted by introducing a residual wetting phase [15]. Respective fluid distributions over the percolating saturation range were the basis for Stokes flow simulations to obtain quasi-static relative permeability. The workflow is sketched in Figure 1. Steady-state relative permeability measurements conducted using Shell's in-house steady-state flow setup with X-ray saturation monitoring [5] were used for validation purpose [2].

RESULTS

During the imbibition experiment, the initially mostly connected non-wetting phase first decreases its internal connectivity through snap-off processes and then breaks apart into clusters of increasing size as displayed in Figure 2A.

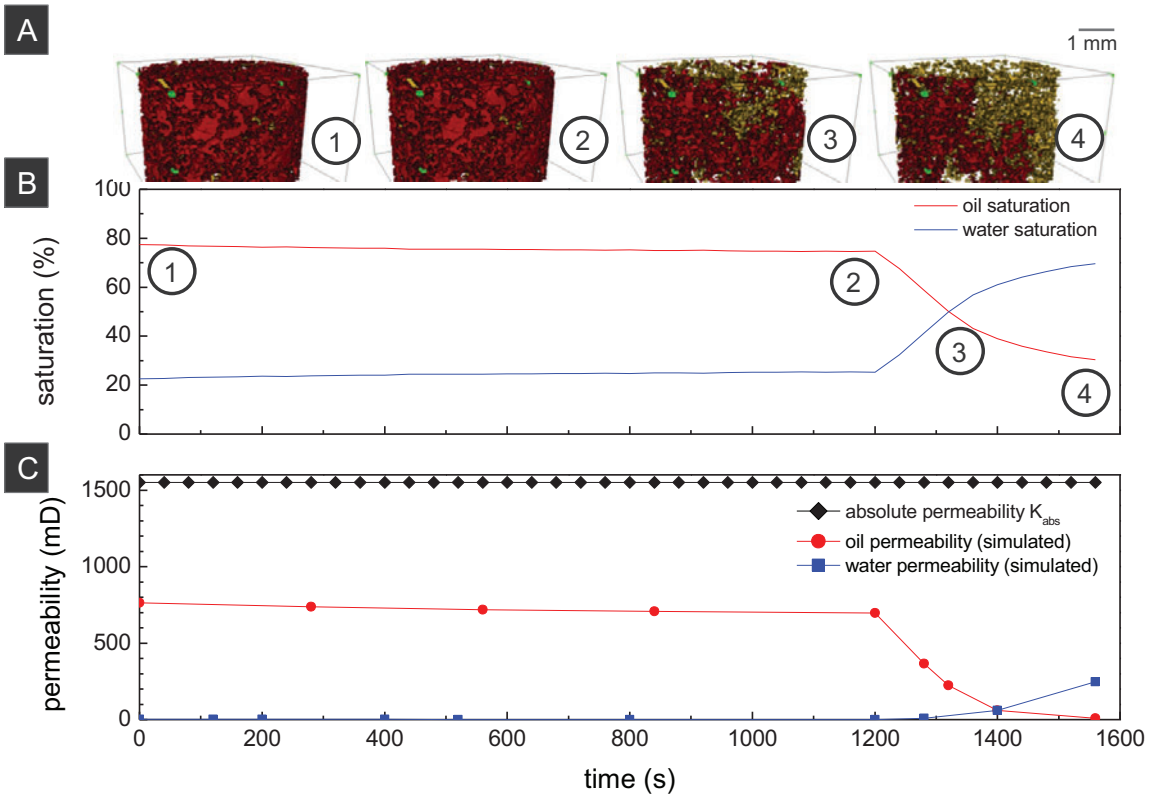

Figure 2: (A) Pore scale fluid of the connected (red) and disconnected (yellow) non-wetting phase during the imbibition experiment. (B) Respective saturation and (C) permeability of wetting and non-wetting phases (reproduced from [1]).

As the non-wetting phase saturation decreases (Figure 2B) the break-up into clusters involves snap-off and coalescence processes of increasing number and magnitude, which – as explained in more detail in [1] – can be summarized as an increasing degree of ganglion dynamics over connected pathway flow. Due to the loss of connectivity, also the connected pathway relative permeability of the non-wetting phase is decreasing while the relative permeability of the wetting phase increases which is displayed in Figure 2C.

Relative Permeability

From the data in Figure 2B and Figure 2C we can now plot the (connected pathway) relative permeability-saturation relationship for the beamline imbibition experiment, which is displayed in **Error! Reference source not found.** on the top panel.

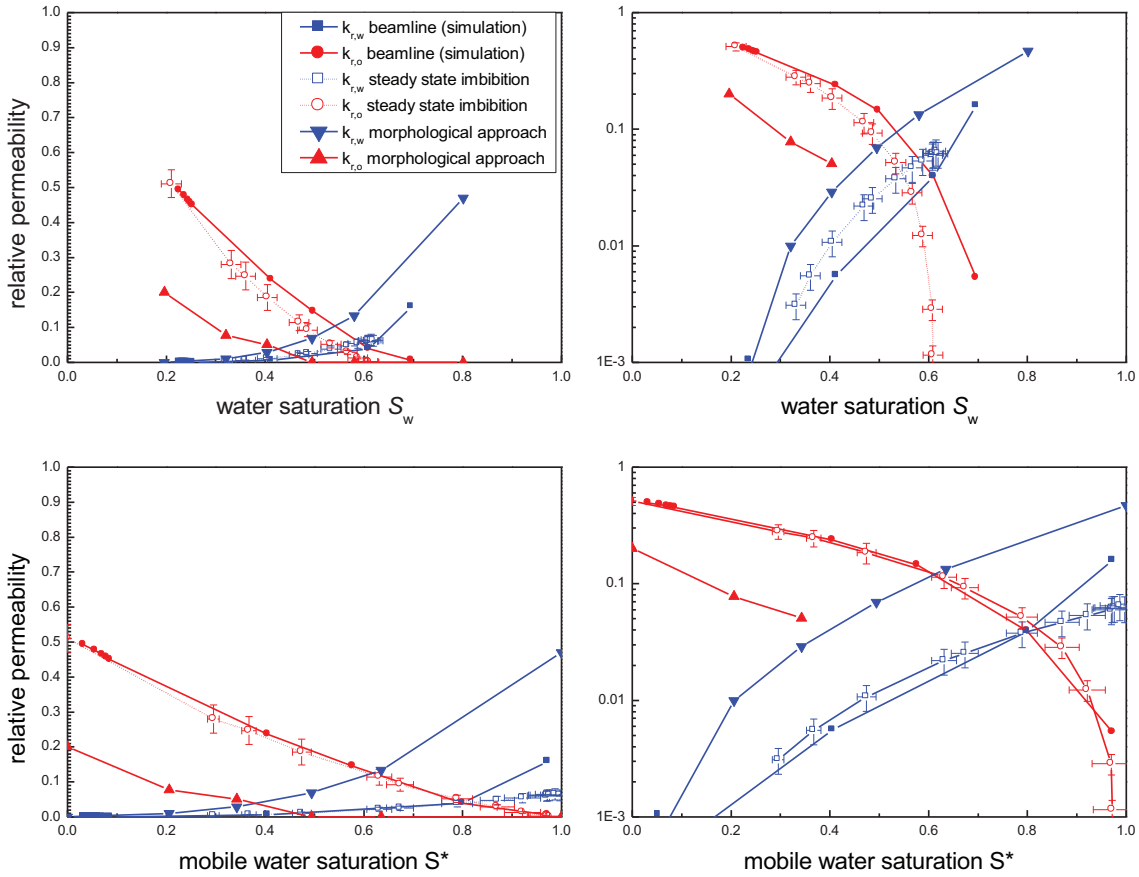

Figure 3: Relative permeability computed from the pore scale fluid distribution in the synchrotron beamline experiment, the morphological approach and the steady-state SCAL data on a linear (left) and logarithmic scale (right) as a function of water saturation S_w (top) and mobile water saturation S^* (bottom).

As a reference we add the relative permeability from the steady-state SCAL data and find that the trends are very similar but that the endpoint saturation (i.e. S_{or}) differs. That can have different reasons, starting from the fact that these are not identical but twin samples, of very different size [2] which could well impact the balance of viscous and capillary

forces over trapped clusters [17]. Therefore the relative permeability data is compared on the basis of the mobile saturation

$$S^* = \frac{S_w - S_{w,c}}{1 - S_{w,c} - S_{o,r}} \quad (1)$$

where $S_{w,c}$ and $S_{o,r}$ are the irreducible wetting and non-wetting phase saturations, respectively. As shown in **Error! Reference source not found.** on the bottom panel the connected pathway relative permeability vs. mobile saturation S^* from the beamline data shows very good agreement with the steady-state SCAL data. This means that for a given pore scale fluid distribution, relative permeability can be sufficiently well computed by considering only the connected pathway contribution (and ignoring the flux of ganglia) over a wide saturation range. That is still very impractical for Digital Rock applications because one would need to measure the pore scale fluid distribution in a synchrotron beamline experiment, which is more effort than conducting a steady-state experiment. Therefore the question arises whether the pore scale fluid distribution of wetting and non-wetting phases can be estimated for instance by a morphological approach.

Capillary Pressure and Relative Permeability from Morphological Approach

As a first step the morphological approach has been validated in drainage against mercury intrusion (MICP) capillary pressure data showing excellent agreement as shown in Figure 4. For comparison, also the scaled water-oil capillary pressure data from the imbibition "simulation" is superimposed which is very close to the drainage data.

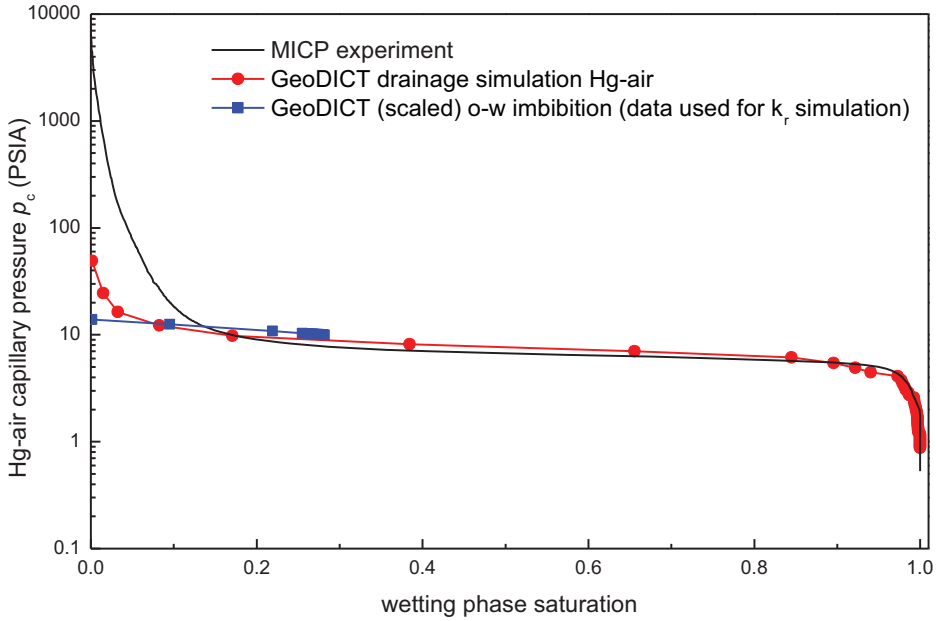

Figure 4: Capillary pressure obtained from mercury intrusion (MICP), the morphological approach in drainage mode and the morphological approach in imbibition mode for the water-oil system (scaled here by interfacial tension and contact angle ratios for comparison).

With respect to the imbibition relative permeability, as **Error! Reference source not found.** clearly shows the data from the morphological approach [13-15] is very different from the SCAL data and the beamline experiment in terms of the percolating saturation range and magnitude of relative permeability for wetting and non-wetting phases. That is not surprising as many pore network modelling studies have shown that imbibition is less approachable than drainage [19]. The underlying reason is that in drainage pore scale displacement processes are mainly Haines jumps which largely maintain connectivity while in imbibition, snap-off processes lead to disconnection and a resulting more complex pore scale fluid topology [21]. That may offer an explanation why in previous studies [16, 20] which are in many respect similar to our work but conducted in drainage instead of imbibition relatively good agreement between the (connected pathway) relative permeability from the quasi-static approach and the one computed on the pore scale fluid configuration in μCT flow experiments.

Pore Scale Fluid Distribution

The discrepancies between the (connected pathway) relative permeability from the μCT flow experiment conducted under dynamic conditions and the quasi-static approach conducted in the capillary limit directly on the pore space originate from a largely different pore scale fluid distribution which is ultimately the consequence of the approach being more applicable for drainage than for imbibition.

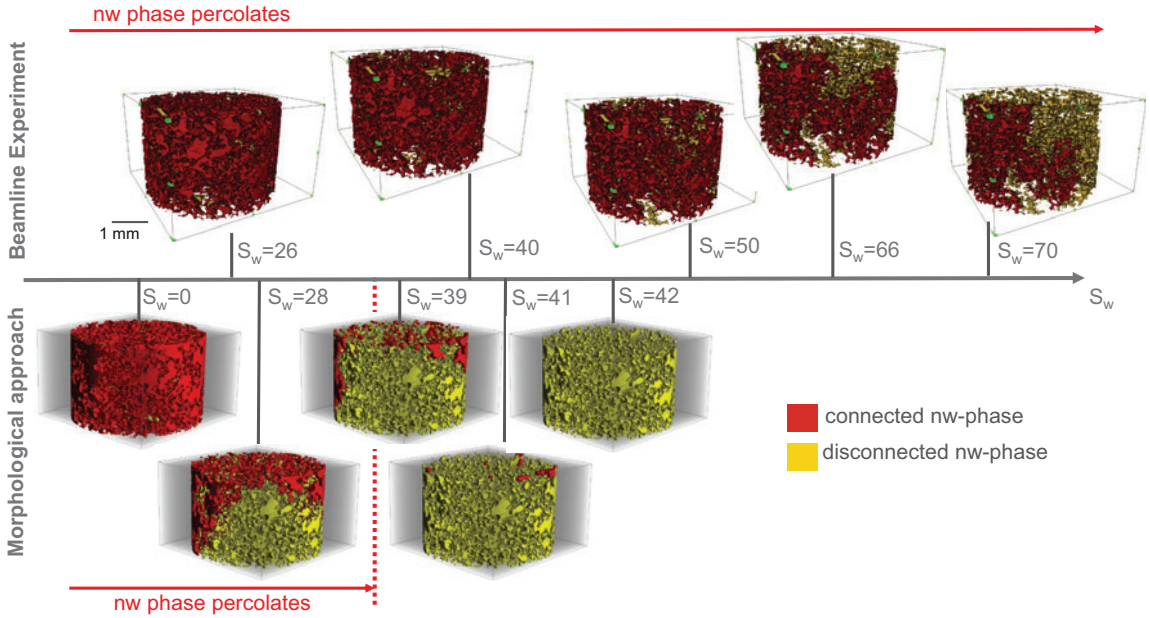

Figure 5: Connected (red) and disconnected (yellow) non-wetting phase for the data from the dynamic synchrotron beamline μCT flow experiment (top) and the morphological approach (bottom) conducted directly on the pore space. The experimental data shows percolation over a much larger saturation range than the morphological approach.

As shown in Figure 5 in the experiment the non-wetting phase percolates over a much larger saturation range than the quasi-static approach predicts. That is consistent with

earlier findings that under dynamic flow conditions, even for capillary numbers based on the injection rate, ganglion dynamics co-exists with connected pathway flow [1]. Ganglion dynamics is composed of snap-off and coalescence which both include capillary and viscous forces. The latter are not present in the quasi-static approach but in reality can during a displacement processes become comparable to capillary forces.
In order to quantify to which degree the pore scale fluid distributions of the morphological approach differ from the experimental data, also in terms of percolation threshold, we compute the Euler characteristic χ as a measure for the topology of the non-wetting phase directly from the pore scale fluid configuration using the image processing software Avizo (FEI). The Euler characteristic is a topological invariant that can be expressed as the difference between the number of objects (zeroth Betti number β_0) and the number of redundant loops [23,24]

$$\chi = \beta_0 - \beta_1 \qquad (2)$$

In Figure 6 the Euler characteristic χ of the experimental data [1] is plotted as a function of wetting phase saturation S_w. For the saturation range of the experiment ($0.22 < S_w < 0.70$), $\chi<0$ which indicates that the non-wetting phase is percolating (in agreement with Figure 5), i.e. consists of more redundant loops (mainly around the grains) than individual clusters. Typically $\chi = 0$ is considered as an indication for the percolation threshold which for the experimental data is expected around S_w~0.7.

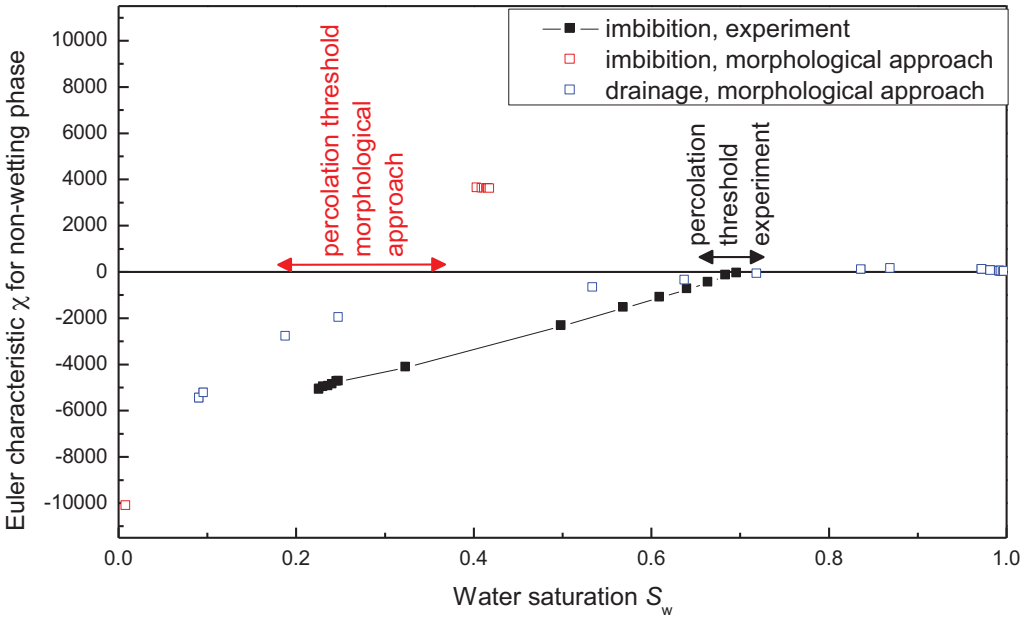

Figure 6: Euler characteristic χ for the non-wetting (oil) phase as a function of water saturation for the imbibition experiment, the fluid configuration obtained from the morphological approach for imbibition (**Figure 1**) and also for drainage. The zero-crossing of χ can be associated with the percolation threshold which is between S_w~0.05-0.3 for the morphological approach and between S_w~0.7-0.8 for the imbibition experiment. In drainage, $\chi \leq 0$ which means that the non-wetting phase always percolates.

For the imbibition data from the morphological approach, on the other hand, the percolation threshold is between $0.2 < S_w < 0.35$ also roughly consistent with Figure 5. Over a large saturation range $\chi>0$ indicating that the pore scale fluid configurations predicted by the (imbibition) morphological approach are non-percolating. Interestingly when applying the morphological approach in drainage mode $\chi \leq 0$ meaning that the non-wetting phase always maintains connectivity, as expected for drainage. Note that the calculation of the Euler characteristic χ is very sensitive to small disconnected clusters that could be noise or segmentation errors in the experimental data, and also artifacts of the morphological approach. Therefore in Figure 6 all clusters smaller than 100 voxels which corresponds to spherical cluster with about 25 μm diameter which is about the noise level in the data, see Fig. 4 in [25]. Rejecting clusters with 50 voxels leads to very similar results.

On the basis of the Euler characteristic as measure for fluid topology we can clearly see also quantitatively that the morphological approach is producing very different pore scale fluid configurations than observed in the experiment. The origin of the differences between the pore scale fluid configuration of the morphological approach and the experimental data relates to ignoring viscous forces (and inertial forces [10]) in modelling pore scale displacement processes by the morphological approach, which operates in the capillary limit. The resulting fluid configurations differ [10] in connectivity, which has a strong impact on transport properties such as the connected pathway relative permeability. Due to the absence of viscous forces, relaxation phenomena and internal fluid re-distribution caused by local capillary pressure gradients is not captured in any quasi-static approach. The associated time scales for relaxation range from seconds [27] to many hours [26]. As a consequence, during 2-phase flow at field relevant flow rates of 1 ft / day, the fluid-fluid interfaces and associated menisci are in reality in most cases not in equilibrium. The quasi-static method, however, always assumes an equilibrium curvature and capillary re-distribution phenomena are not captured. These, however, may play a relevant role for the pore scale fluid configuration.

This work shows also that the flux contribution of ganglion dynamics is more of a secondary effect but can become significant close to residual saturation as a recent lattice Boltzmann study shows [18,30].

With all the simplifications and approximations the quasi-static approach is more applicable to drainage. The drainage capillary pressure-saturation relationship is described very well by the morphological approach. However the (scaled) imbibition capillary pressure is very similar to the drainage capillary pressure which is a first indication that the morphological approach, even if executed in “imbibition mode” reflects overall more of a drainage process. Also the resulting relative permeability is closer to drainage steady-state data [2].

CONCLUSIONS AND OUTLOOK

The way how we start looking at multiphase flow on the pore scale is that the only aspect that is capillary dominated is the flow regime where fluid interfaces remain static, which is commonly termed “connected pathway flow”. Direct imaging of pore scale flow

experiments by tomography clearly shows that pore scale displacement events are cooperative [1,28] and fast [10,27], non-local processes involving many pores which is conceptually different than simple percolation models and quasi-static pore network models predict. In particular in imbibition we find a complex interaction between film swelling and corner film flow and the breakup of clusters. When following the transition from a connected phase flow to individual clusters, at the onset of oil mobilization which occurs at relatively large oil saturation, the main mechanism is snap-off leading to a breakup of clusters [1]. The large meniscus oscillations initiated by the snap-off, on the other hand, also leads to coalescence events, which again points to the cooperative dynamics in the ganglion dynamics regime [1,18]. In this way transport occurs over a larger saturation range than in direct quasi-static approaches. Apparently this also causes connectivity of the non-wetting phase being maintained over a larger saturation range. The morphological approach, on the other hand, shows percolation of the non-wetting phase over a smaller saturation range than the experiments.

It is important to note that the direct quasi-static approaches currently lack the sophistication in term of rule-based displacement mechanisms as for instance quasi-static pore network models. Therefore it is not fully clear whether pore network models would create a better match with the experimental data. Future research on this matter may answer this question. However it is important to tune the networks only in a very moderate way to ensure that a one-to-one correspondence to the pore space is maintained. Conversely direct quasi-static approaches are currently being extended by similar displacement rules as network models to improve the accuracy of the pore scale saturation distribution.

ACKNOWLEDGEMENTS

Ton Blok is gratefully acknowledged for the MICP measurements. Sebastiaan Pieterse and Niels Brussee are gratefully acknowledged for the steady-state relative permeability measurements. Fons Marcelis and Ab Coorn are acknowledged for sample preparation and Soxhlett cleaning. We acknowledge the Paul Scherrer Institut, Villigen, Switzerland for provision of synchrotron radiation beamtime at the TOMCAT beamline of the SLS and would like to thank Sally Irvine and Marco Stampanoni for assistance.

REFERENCES

1. M. Rücker, S. Berg, R. T. Armstrong, A. Georgiadis, H. Ott, A. Schwing, R. Neiteler, N. Brussee, A. Makurat, L. Leu, M. Wolf, F. Khan, F. Enzmann, M. Kersten, From connected pathway flow to ganglion dynamics, Geophys. Res. Lett. 42, 3888–3894, 2015.
2. S. Berg, M. Rücker, H. Ott, A. Georgiadis, H. van der Linde, F. Enzmann, M. Kersten, R. T. Armstrong, S. de With, J. Becker, A. Wiegmann, Connected Pathway Relative Permeability from Pore Scale Imaging of Imbibition, Advances in Water Resources 90, 24-35, 2016.
3. C. W. Dubelaar, T. G. Nijland, Early cretaceous Obernkirchen and Bentheim sand-stones from Germany used as dimension stone in the Netherlands: geology, physical

properties, architectural use and comparative weathering. Geol Soc Lond 416, 416–513, 2015.
4. N. Evseev, R. T. Armstrong, S. Berg, O. Dinariev, D. Klemin, D. Koroteev, S. Safonov, Modeling of pore-scale two-phase flow phenomena using density functional hydrodynamics, Transport in Porous media, DOI:10.1007/s11242-016-0660-8, 2016.
5. J.A. Kokkedee, W. Boom, A.M. Frens, Improved special core analysis: scope for a reduced residual oil saturation. Society of core analysis conference paper, 9601; 1996.
6. S.Berg, H. Ott, S. A. Klapp, A. Schwing, R. Neiteler, N. Brussee, A. Makurat, L. Leu, F. Enzmann, J.-O. Schwarz, M. Kersten, S. Irvine, M. Stampanoni, Real-time 3D imaging of Haines jumps in porous media flow. Proc Natl Acad Sci 10, 3755–9, 2013.
7. S. Youssef, E. Rosenerg, H. Deschamps, R. Oughanem, E. Maire, R. Mokso, Oil ganglia dynamics in natural porous media during surfactant flooding captured by ultra-fast x-ray microtomograph. International symposium of the society of core analyst, Avignon, France, 11–18 September, 2014; SCA2014–23.
8. M. J. Blunt, M. D. Jackson, M. Piri, P. H. Valvatne, Detailed physics, predictive capabilities and macroscopic consequences for pore-network models of multiphase flow. Adv Water Resour 25, 1069–89, 2002.
9. V. Joekar-Niasar, S. M. Hassanizadeh. Uniqueness of specific interfacial area–capillary pressure–saturation relationship under non-equilibrium conditions in two-phase porous media flow. Transp Porous Media 94, 465–86, 2012.
10. A. Ferrari, I. Lunati, Direct numerical simulations of interface dynamics to link capillary pressure and total surface energy. Adv Water Resour 57, 19–31, 2013.
11. A. Q. Raeini, M. J. Blunt, B. Bijeljic, Direct simulations of two-phase flow on micro-CT images of porous media and upscaling of pore-scale forces. Adv Water Resour 74, 116–26, 2014.
12. D. Koroteev, O. Dinariev, N. Evseev, D. Klemin, A. Nadeev, S. Safonov, O. Gurpinar, S. Berg, C. van Kruijsdijk, R. Armstrong, M. T. Myers, L. Hathon, H. de Jong, Direct Hydrodynamic Simulation of Multiphase Flow in Porous Rock, Petrophysics 55(4), 294–303, 2014.
13. M. Hilpert, T. C. Miller, Pore-morphology-based simulation of drainage in totally wetting porous media. Adv Water Resour 24, 243–55, 2001.
14. H. J. Vogel, J. Tölke, VP Schulz, M Krafczyk, K Roth, Comparison of a lattice-Boltzmann model, a full morphology model, and a pore network model for determining capillary pressure-saturation relationships. Vadose Zone J 4, 380–8, 2005.
15. J. Becker, V. Schulz, A. Wiegmann, Numerical determination of two-phase material parameters of a gas diffusion layer using tomography images. J. Fuel Cell Sci. Tech. 5, 2008.
16. F. Hussain, W. V. Pinczweski, Y. Cinar, J. Y. Arns, C. H. Arns, M. L. Turner, Computation of relative permeability from imaged fluid distributions at the pore scale. Transp Porous Med 104, 91–107, 2014.

17. R. T. Armstrong, A. Georgiadis, H. Ott, D. Klemin, S. Berg, Pore-scale mobilization of non-wetting phase ganglia and critical capillary number for onset of macroscopic capillary desaturation. Geophys Res Lett 41, 1–6, 2014.
18. R. T. Armstrong, J. E. McClure, M. A. Berrill, M. Rücker, S. Schlüter, S. Berg, Beyond Darcy's law: The Role of Phase Topology and Ganglion Dynamics for Two Fluid Flow, submitted, 2016.
19. G. Mason, N. R. Morrow, Developments in spontaneous imbibition and possibilities for future work. J Pet Sci Eng 110, 268–93, 2013.
20. M. Turner, L. Knüfing, C. Arns, A. Sakellariou, T. Senden, A. Sheppard, R. Sok, A. Limaye, W. V. Pinczewski, M. Knackstedt, Three-dimensional imaging of multiphase flow in porous media. Physica A 339, 166–72, 2004.
21. S. Schlüter, S. Berg, M. Rücker, R. T. Armstrong, H.-J. Vogel, R. Hilfer, D. Wildenschild, Pore scale displacement mechanisms as a source of hysteresis for two-phase flow in porous media, Water Resources Research, *in press*, 2016.
22. B. Raeesi, N. Morrow, G. Mason, Pore network modeling of experimental capillary pressure hysteresis relationships. International symposium of the society of core analysts held in Napa Valley. California, USA, 16–19 September 2013, SCA2013-015.
23. A. L. Herring, E. J. Harper, L. Andersson, A. Sheppard, B. K. Bay, D. Wildenschild, Effect of fluid topology on residual nonwetting phase trapping: Implications for geologic CO2 sequestration, Adv. Water Resour. 62, 47–58, 2013.
24. S. Schlüter, A. Sheppard, K. Brown, D. Wildenschild, Image processing of multiphase images obtained via X-ray microtomography: A review, Water Resour. Res. 50, 3615–3639, 2014.
25. S.Berg, R. T. Armstrong, A. Georgiadis, H. Ott, A. Schwing, R. Neiteler, N. Brussee, A. Makurat, M. Rücker, L. Leu, M. Wolf, F. Khan, F. Enzmann, M. Kersten, Onset of Oil Mobilization and Non-Wetting Phase Cluster Size Distribution, SCA2014-022, 2014.
26. S. Schlüter, T. Li, H.-J. Vogel, S. Berg, D. Wildenschild, Different time scales of relaxation dynamics during hydraulic non-equilibrium in two-phase flow, *in preparation*.
27. R. T. Armstrong, H. Ott, A. Georgiadis, M. Ruecker, A. Schwing, S. Berg, Sub-second pore scale displacement processes and relaxation dynamics in multiphase flow, Water Resources Research, DOI: 10.1002/2014WR015858, 2014.
28. R. T. Armstrong, N. Evseev, D. Koroteev, S. Berg, Modeling the velocity field during Haines jumps in porous media, Advances in Water Resources 77, 57-68, 2015.
29. B. Ahrenholz, J. Tölke, P. Lehmann, A. Peters, A. Kaestner, M. Krafczyk, W. Durner. Prediction of capillary hysteresis in a porous material using lattice-Boltzmann methods and comparison to experimental data and a morphological pore network model. Advances in Water Resources 31, 1151–1173, 2008.
30. R. T. Armstrong, J. E. McClure, M. A. Berill, M. Rücker, S. Schlüter, S. Berg, Flow Regimes During Immiscible Displacement, SCA 2016.